Food Hydrocolloids 172 (2026) 112189

Contents lists available at ScienceDirect

Food Hydrocolloids

journal homepage: www.elsevier.com/locate/foodhyd

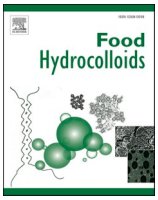

Gelation of methylcellulose-protein mixtures: effect of methylcellulose molecular weight and protein characteristics

Thiemo van Esbroeck [a], Guido Sala [a], Markus Stieger [b,c], Elke Scholten [a,*]

[a] Physics and Physical Chemistry of Foods, Wageningen University & Research, Bornse Weilanden 9, 6708WG, Wageningen, Netherlands
[b] Division of Human Nutrition and Health, Wageningen University & Research, Bornse Weilanden 9, 6708WG, Wageningen, Netherlands
[c] Food Quality and Design, Wageningen University & Research, Bornse Weilanden 9, 6708WG, Wageningen, Netherlands

ARTICLE INFO

Keywords:
Plant protein
Microstructure
Phase separation
Syneresis
Rheology
Meat analogues

ABSTRACT

Methylcellulose (MC) is a widely used functional ingredient due to its thermo-reversible gelation properties, which is particularly important in applications such as meat analogues. Since these products have a high protein content, understanding the gelation behaviour of MC-protein mixtures is essential. This study investigated the gelation of MC-protein systems using methylcelluloses with molecular weights ranging from 100 to 300 kg/mol and two distinct protein isolates; pea protein isolate (PPI), a denatured and aggregated protein, and potato protein isolate (PoPI), a native and highly soluble protein. Confocal microscopy revealed that addition of PPI to MC resulted in MC gels in which PPI was present as microphase-separated domains that became more interconnected with increasing PPI concentration. PPI addition did not influence the mechanical properties of the gels, but strongly impacted the syneresis of the gels, which increased significantly—up to 10 wt%. Syneresis was more pronounced for MCs with higher molecular weight due to the formation of denser network structures upon contraction, leading to more expelled liquid. This syneresis was amplified by the presence of interconnected PPI domains resulting from the microphase separation. In systems with low PoPI concentrations, the protein acted as a dispersed phase within an MC matrix, without altering the gel moduli. However, at sufficiently high PoPI concentration (7.5 wt%), the protein formed its own space-spanning network next to that of MC, leading to a synergistic increase in gel strength—up to a threefold enhancement. This enhanced gel strength likely stemmed from increased effective concentrations of MC and PoPI, as well as hydrophobic interactions between MC and PoPI within the networks. MCs with lower molecular weight formed less interconnected networks, which resulted in a more pronounced contribution of PoPI to the gel moduli. MC gels containing PoPI did not exhibit syneresis due to the water-retaining capacity of the protein network. We conclude that protein characteristics have a broad impact on the structural, mechanical and syneresis properties of MC-protein gels, whereas the molecular weight of MC primarily affects syneresis.

1. Introduction

Methylcellulose (MC) is a water-soluble polysaccharide derived from cellulose that exhibits unique thermo-reversible gelation behaviour. This behaviour has contributed to widespread use in ceramics, pharmaceutical and food applications (Chen et al., 2006; Liu et al., 2004; Nasatto et al., 2015; Sandoval & Camerucci, 1979, 2017; Tate et al., 2001; Whistler & BeMiller, 1992). One of the main food applications of MC is in meat analogues, in which its gelation upon heating ensures the structural integrity and firmness of these products during cooking. Additionally, MC helps to bind water, can reduce cooking loss, and its melting behaviour during consumption as a result of a decrease in temperature may positively impact sensory perception (Hill & Prusa, 1988; Kyriakopoulou et al., 2021; Whistler & BeMiller, 1992).

The specific thermo-reversible gelation behaviour of methylcellulose arises from its molecular structure. Methylcellulose is a cellulose ether with hydroxyl groups that are partially substituted with methoxy groups, typically achieving a degree of substitution between 1.7 and 2.0 to ensure good water solubility (Arvidson et al., 2013; Chatterjee et al., 2012; Fairclough et al., 2012; Li et al., 2001; McAllister, Lott, et al., 2015; Nasatto et al., 2015; Schmidt et al., 2018; Wang et al., 2006). At low temperatures, MC is soluble in water due to the formation of

* Corresponding author.
E-mail address: elke.scholten@wur.nl (E. Scholten).

https://doi.org/10.1016/j.foodhyd.2025.112189
Received 29 May 2025; Received in revised form 29 October 2025; Accepted 30 October 2025
Available online 1 November 2025

hydrogen bonds with water molecules. Upon heating, these hydrogen bonds weaken, allowing MC chains to associate into fibrils that form a gel network stabilised by increased hydrophobic interactions (Bodvik et al., 2010; Lott, McAllister, Arvidson, et al., 2013; Schmidt et al., 2020). This gelation process is thermally reversible and exhibits hysteresis (Schmidt et al., 2018), meaning that the temperature required for MC to resolubilise is lower than the gelation temperature (T_g). Many recent studies investigated the fibril formation of MC and the subsequent formation of a gel network (Bodvik et al., 2010; Coughlin et al., 2021; Liberman et al., 2021; Lott, McAllister, Wasbrough, et al., 2013; McAllister et al. 2015a, 2015b; Schmidt et al., 2018, 2020). Previous research has established that, during heating, MC forms fibrils with a diameter of ~15–20 nm and a Kuhn length of ~50 nm, which are independent of MC concentration, molecular weight and the regularity of methoxy substitution. These parameters have an influence on the structural and rheological characteristics of MC gels. For example, at a fixed MC concentration, G′ increases with molecular weight, which can be attributed to the formation of longer fibrils and a more connected fibrillar network (Schmidt et al., 2018).

While understanding the gelation behaviour of MC systems is important, meat analogues and other applications often involve mixing of MC with other ingredients, such as proteins, polysaccharides, salts, and surfactants. Comprehending how these components affect MC gelation and structure formation is critical for optimising MC performance in more complex systems. In this context, various studies have explored the effect of salt on MC gelation (Kundu & Kundu, 2001; Kundu & Singh, 2008; Li et al., 2007; Sarkar, 1979; Thirumala et al., 2013; Xu et al., 2004; Zheng et al., 2004). Generally, salting-in and salting-out effects were found to respectively increase and decrease the gelation temperature, respectively (Kundu & Kundu, 2001; Li et al., 2007; Sarkar, 1979; Xu et al., 2004; Zheng et al., 2004). These effects can be modulated by selecting the appropriate salt type and concentration. Xu et al. (2004) reported that salting-out enhanced gel strength, whereas salting-in had no effect on gel strength. MC has also been combined with a variety of polysaccharides, such as alginate (Liang et al., 2004; Schütz et al., 2017; Shimoyama et al., 2012), agarose (Martin et al., 2008), xanthan (Liu & Yao, 2015) and carrageenan (Almeida et al., 2018; Tomšič et al., i2008, 2009). These are all cold-gelling polysaccharides, leading to unique double-gelling behaviour of such mixtures. For example, Liu and Yao (2015) demonstrated that MC-xanthan mixtures comprised interpenetrating MC and xanthan networks, allowing to tune gel properties by changing polysaccharide concentration and ratio. In contrast, Tomšič et al. (2008) showed that MC and carrageenan can also form independent networks, and that the components do not interfere with each other during gelation and solubilisation.

While the influence of salts, surfactants and polysaccharides on MC gelation has received considerable attention, research on MC-protein mixtures remains scarce, despite their importance in applications like meat analogues. He et al. (2022) explored the interactions between MC and soy protein, revealing hydrophobically-driven aggregation between these two components at room temperature. Upon heating, a more heterogeneous network with larger aggregates was observed, resulting in less elastic gels compared to those formed by MC only. In a more recent study, Ryu and McClements (2024) explored the effects of MC on the gelation of potato protein. They reported that the potato protein dominated the gelation process, with MC causing only minor interference. Furthermore, the addition of MC lowered the denaturation temperature of potato protein slightly, which was proposed to be due to hydrophobic interactions between MC and protein. While these two studies (He et al., 2022; Ryu & McClements, 2024) provide insights into MC-protein interactions and their impact on gelation, they focussed on single MC and protein types. The effects of MC molecular weight, protein type and characteristics, and protein concentration on the gelation of MC-protein mixtures, as well as their structural organisation as a function of temperature, have not been reported previously.

The aim of this study was to systematically evaluate the effect of MC molecular weight and protein characteristics on the structural and mechanical properties of MC-protein gels. We employed MCs with four molecular weights ranging from 100 to 300 kg/mol, consistent with ranges commonly used in literature to study MC gelation under comparable conditions. Two distinct proteins were selected to represent specific conditions. Potato protein was chosen as a representative of a plant protein with high nativity and solubility, whereas pea protein was selected to represent a plant protein with low functionality, characterised by a highly denatured and aggregated state, resulting in low solubility. Various analytical techniques, such as particle size analysis, differential scanning calorimetry (DSC), shear rheology, and temperature-controlled confocal laser scanning microscopy (CLSM) were used to gain insights into the gelation behaviour of MC-protein mixtures and the resulting structural organisation. The findings of this study may contribute to enhancing the functional performance of methylcellulose-protein systems in applications like meat analogues.

2. Materials and methods

2.1. Materials

For the preparation of the MC-protein mixtures, four types of methylcellulose and two protein isolates from different origin were used. Metolose MCE-100, MCE-400, MCE-1500 and Tylopur MCE-4000, with viscosities (2 wt% solutions at 20 °C) of 100, 400, 1500 and 4000 mPa s, respectively, were kindly provided by Shin-Etsu Chemicals Co., Ltd. (Chiyoda-ku, Tokyo, Japan). These MCs had weight-average molecular weights (M_w) of 100, 140, 210 and 300 kg/mol, and are referred to in this study by their M_w as MC100, MC140, MC210 and MC300. The methoxyl content of all MC types was similar, ranging from 29.4 % to 30.9 %. Potato protein isolate (PoPI, Solanic 200) was purchased from Avebe (Veendam, The Netherlands) and yellow pea protein isolate (PPI, NUTRALYS® S85XF) was obtained from Roquette Frères S.A. (Lestrem, France). Rhodamine B (Sigma-Aldrich, Saint Louis, Missouri, USA) and Calcofluor White, specifically the formulation without Evans blue (Biotium, Fremont, California, USA), were used as fluorescent dyes for confocal laser scanning microscopy. Ultrapure water, purified by a Millipore Milli-Q system (Darmstadt, Germany), was used for all experiments.

2.2. Sample preparation

Stock solutions of 4 wt% MC were prepared by dispersing MC in water at 60 °C while stirring. Stock solutions of 15 wt% PPI or PoPI were obtained by stirring dispersions for 4 h at room temperature. These dispersions were allowed to hydrate in the fridge for at least 12 h, after which they were combined and mixed using an overhead stirrer for 10 min at 2000 rpm. Final concentrations of the MC-protein mixtures were 2 wt% MC and 2.5, 5 and 7.5 wt% protein. Air bubbles induced by mixing were removed by centrifugation at 1000*g* for 1 min for samples with MC100 and MC140, and for 3 min for samples with MC210 and MC300.

2.3. Methods

2.3.1. Protein content

To determine the protein concentration of the protein isolates, the elemental nitrogen content was determined using the Dumas method. Nitrogen concentrations were determined during combustion in a Flash EA 1112 N/protein analyzer (Thermo Fisher Scientific, Waltham, Massachusetts, USA). Conversion factors of 5.60 (Hinderink et al., 2021) and 6.25 (Van Gelder, 1981) were used for pea and potato protein, respectively, to convert the nitrogen content to protein content, which is expressed on dry matter basis. Measurements were done in triplicate.

2.3.2. Particle size distribution

The particle size of PPI and MC-PPI mixtures was measured with static light scattering using a Mastersizer 3000 coupled with a Hydro MV dispersion unit (Malvern Instruments Ltd., Worcestershire, UK). Samples were added into the dispersion unit to an obscuration of 5–10 %. The stirring speed was set to 3000 rpm. Volume-weighted size distributions were determined using the Mie scattering theory. The refractive indices used for the dispersed phase (pea protein) and dispersant (ultrapure water) were 1.45 and 1.33, respectively, and the adsorption index was set to 0.001. For MC-PPI mixtures, a refractive index of 1.45 was used for the dispersed phase. Mean sizes reported are volume-weighted mean diameters ($d_{4,3}$). Measurements were performed in triplicate at room temperature.

Given the distinct particle size ranges of PPI, MC and PoPI, the use of two different instruments was necessary. Hence, the size of PoPI, the four different types of MC, and MC-PoPI mixtures was determined using dynamic light scattering in a Zetasizer Nano ZS (Malvern Instruments, Malvern, UK) with a He-Ne laser with a wavelength of 632.8 nm, and a photodiode detector with a detection angle of 173°. Samples containing only protein or MC were prepared at 0.1 wt%. The MC-PoPI mixtures were prepared at 0.2 wt% MC and 0.25, 0.50 or 0.75 wt% PoPI. All samples were filtered through a 0.45 μm syringe membrane filter to remove any insoluble material. Ultrapure water was used as dispersant with a refractive index of 1.330. The refractive indices used were 1.45 for proteins, 1.44 for MC, and 1.45 for the MC-PoPI mixtures. The absorption index for PoPI and MC were both 0.001. For samples containing MC, viscosity was measured according to section 2.3.6, and we verified that it had negligible impact on the size measurements. Therefore, the viscosity of the PoPI and MC-PoPI solutions was set to the default value of 0.89 mPa s for water. Samples were loaded in a polystyrene cuvette (67.742, Sarstedt AG & Co. KG, Nümbrecht, Germany). Before each measurement, the sample was equilibrated for 1 min. Each sample was measured in triplicate at 20 °C, and each replicate consisted of 3 sub-measurements. The volume-weighted average hydrodynamic diameter was calculated by the ZS Xplorer software (version 2.3.1.4) by cumulant analysis using the general purpose model.

2.3.3. Zeta-potential

The ζ-potential of PPI, PoPI and four different types of MC were determined using dynamic light scattering in a Zetasizer Nano ZS (Malvern Instruments, Malvern, UK). Protein and MC samples contained 0.1 wt% protein and 1 wt% MC, respectively. Samples were filtered through a 0.45 μm syringe membrane filter to remove any insoluble material. Ultrapure water was used as dispersant with a refractive index of 1.330. The cell type was DTS1070 and the refractive indices used were 1.45 for proteins and 1.44 for MC. Before each measurement, the sample was equilibrated for 1 min. All measurements were performed in triplicate at 20 °C.

2.3.4. Thermal characteristics

Thermal properties of MCs, proteins and their mixtures were determined using differential scanning calorimetry (DSC) (DSC25, TA instruments Discovery, Asse, Belgium). Approximately 15 μg of each sample was encapsulated into a hermetically sealed aluminium DSC pan. Nitrogen gas (N_2) inside the heating chamber was used at a rate of 20.4 mL/min. To study the degree of protein denaturation, protein samples were equilibrated at 20 °C for 5 min, heated from 20 °C to 130 °C at a rate of 2 °C/min and the endothermic enthalpy (ΔH, J/g) of the denaturation peak was determined using Trios software version 2.0. To investigate the thermal transitions of MC and MC-protein mixtures, the samples were equilibrated at 10 °C for 5 min, heated from 10 °C to 80 °C at a rate of 2 °C/min and the endothermic and exothermic enthalpy (ΔH, J/g) of the peaks was determined. Measurements were performed in duplicate.

2.3.5. Confocal laser scanning microscopy

The microstructures of the MC, protein and MC-protein mixtures were investigated using a confocal microscope (Zeiss LSM 510 META, Carl Zeiss AG, Oberkochen, Germany) with a rescan-confocal microscopy (RCM) module (Confocal.nl, Amsterdam, The Netherlands), fitted with a 20x air objective lens (Plan Apo, NA = 0.75, WD = 1.0 mm, Nikon, Tokyo, Japan) and a Tucsen FL 20BW CCD camera. During image acquisition, a 2736 × 1824 pixel region was recorded, which translated to an image of 443 × 295 μm (effective pixel size: 162 × 162 nm). To 1 mL of sample, 20 μL of 5 mM aqueous calcofluor-white (CFW) solution was added to stain methylcellulose, and 20 μL of 0.01 wt% Rhodamine B (RhB) aqueous solution to stain proteins. The samples and dye solution were mixed with a spatula, after which air was removed by centrifugation at 1000*g* for 1 min, and subsequently stored at 4 °C for 4 h. The samples were loaded in Smart Substrates (SmSL-R 16, Standard Range, Interherence GmbH, Erlangen, Germany), which were connected to a VAHEAT micro-heating system (v1.2.0, Interherence GmbH, Erlangen, Germany) used for dynamic temperature control during the measurements. The heating and cooling rate was 10 °C per min. CFW was excited at 405 nm at 30 % of the maximum laser power (Oxxius LC4c laser), and RhB was excited at 561 nm at 5 % of the maximum laser power. All images were taken 10 μm from the base of the glass to avoid boundary anomalies in the gel formation, which did not persist beyond 5 μm from the glass surface. Images were acquired with an exposure time of 10 ms at 20 °C, at 70 °C and after cooling again at 20 °C.

For the determination of volume fraction, domain size and domain connectivity, images were processed using a custom Python code. A median filter with a kernel size of 3 pixels (0.5 μm) for MC and MC-PoPI samples, or 9 pixels (1.5 μm) for MC-PPI samples was applied to the image to reduce noise. The image was then binarised using a manually adjusted colour threshold. The volume fraction of MC and protein was calculated as the fraction of pixels of that phase of the total pixel count. A distance map was created for both phases, containing the shortest distance to the other phase, for each pixel. The local maxima in this distance map were analysed. The minimum size of identified objects was set to three times the kernel size for image smoothing. The mean and standard deviation of the local maxima, multiplied by two to obtain the diameter, was taken as the domain size of the system. The processed images were further subjected to connectivity analysis using AngioTool 64 (National cancer Institute, National Institute of Health, Maryland, USA). For each confocal image, the MC and protein phase were analysed separately, producing a series of network parameters including number of junctions and number of end points. The connectivity of MC and protein domains was defined as the number of junctions divided by the number of end points. For each sample, at least four images were analysed.

2.3.6. Rheological properties of MC-protein mixtures

The rheological properties of MC-protein mixtures were measured using a rotational rheometer (Anton Paar MCR302, Anton Paar GmbH, Graz, AT) equipped with a Peltier element, Peltier hood, and a sand-blasted plate-plate geometry (PP50/S/SS – 25400). Shear viscosity (η) was measured as a function of shear rate ($\dot{\gamma}$) using a range from 0.01 to 1000 s^{-1} in a logarithmic fashion at 20 °C. To ensure steady-state conditions at each applied shear rate, the measurement duration for each data point was adjusted logarithmically, starting with 20 s at the lowest shear rate ($\dot{\gamma} = 0.01\ s^{-1}$) and gradually decreasing to 1 s at the highest shear rate ($\dot{\gamma} = 1000\ s^{-1}$). The zero-shear viscosity (η_0) was determined by fitting the experimental viscosity curves with the Carreau-Yasuda model (Yasuda et al., 1981):

$$\frac{\eta}{\eta_0} = \left[1 + (\lambda\dot{\gamma})^a\right]^{\frac{n-1}{a}} \quad (1)$$

where λ is the relaxation time, a is a parameter describing the transition between the zero-shear viscosity and the power-law region, and n is the

power law index.

The linear viscoelastic (LVE) regime of the gels was determined using amplitude sweeps (frequency f = 10 rad/s, strain γ = 0.001–100 %, temperature T = 70 °C). The end of the LVE was defined as the point where the storage modulus (G′) deviated more than 5 % from its strain-independent plateau value within the LVE. The temperature of 70 °C was chosen as it is above the gelation temperature of MC (≈60 °C), ensuring fully gelled samples and reflecting typical processing conditions for applications such as meat analogues. To study the temperature-dependent behaviour of the gels, temperature sweeps were performed within the LVE at a shear amplitude of 0.5 % and an angular frequency of 10 rad/s. To minimise evaporation during the measurements, the sample edges were coated with low-viscosity silicon oil, and a solvent trap was used. The temperature was set to increase from 20 °C to 70 °C at a rate of 1.67 °C/min, which provided sufficient resolution of temperature-dependent changes while preventing evaporation during heating. The temperature was held at 70 °C for 10 min and then decreased to 20 °C at a rate of 1.67 °C/min. The sample was then held at 20 °C for 30 min. All measurements were performed in duplicate.

2.3.7. Syneresis of MC-protein gels

To determine the degree of syneresis of the samples during gelation, MC-PPI and MC-PoPI mixtures (125 mL) were transferred to a 250 mL beaker glass with an inner diameter of 66 mm, resulting in a sample height of 38 mm. The beakers were covered with aluminium foil and heated for 1 h in a water bath preheated to 70 °C. Immediately after heating, the expelled liquid was decanted. The gels were loosened from the edge of the beaker with a spatula, to also decant the liquid expelled below the gel. Syneresis was defined as the percentage of liquid expelled from the gel relative to the initial weight of the sample. Part of the expelled liquid was dried in an oven (Venticell, BMT Medical Technology, Brno, Czech Republic) at 105 °C to determine the dry matter content in the expelled liquid. The other part was used to determine the particle size in the expelled liquid according to the method described in section 2.3.2. All measurements were performed in duplicate.

2.3.8. Textural properties of MC-protein gels

Displacement-controlled indentation tests were performed with a Texture Analyzer (TA-XT plus, Stable Micro Systems Ltd., Godalming, UK) to determine the textural properties of the gels. Preliminary experiments showed that MC-PPI gels melted rapidly when removed from a syringe or beaker, prior to compression. Therefore, MC-PPI and MC-PoPI gels were subjected to an indentation test in situ within a 250 mL beaker glass (gel diameter: 66 mm, gel height: 38 mm). When syneresis was obtained, the expelled liquid was first decanted. The Texture Analyzer was equipped with a 10 kg load cell and a cylindrical polycarbonate probe with a diameter of 30 mm was used to deform the gels with a speed of 1 mm/s and a trigger force of 10 g, and the data up to 10 % strain was used for analysis. During the measurement, the force (F) required to indent the sample was recorded. The nominal indentation stress (σ) was calculated using force and area of the probe (A) using $\sigma = F/A$. All measurements were performed in duplicate.

2.4. Statistical data analysis

Unless stated otherwise, all results are presented as mean ± standard deviation of independent replicates. The effects of methylcellulose (MC) molecular weight, protein type and protein concentration on the onset temperature (T_{onset}), peak temperature (T_{peak}), enthalpy (ΔH), zero-shear viscosity (η_0), connectivity of MC- and protein-rich domains, storage modulus at 70 °C and the nominal indentation stress were assessed using a three-way MANOVA followed by Tukey post-hoc analyses. MC molecular weight, protein type, protein concentration and their interactions were treated as fixed factors. For the storage modulus at 20 °C and syneresis, for which only MC molecular weight and protein concentration were relevant, two-way ANOVA was applied, in which MC molecular weight, protein concentration and their interaction were treated as fixed factors. Data of reference samples, such as pure protein solutions, were excluded from the statistical analysis. All statistical analysis were conducted in RStudio (version 2022.07.0, PBC) using the package emmeans (Lenth, 2022) with a significance level of $p < 0.05$.

3. Results & discussion

3.1. Material characterisation

3.1.1. Particle size distribution

The average volume-weighted size distribution of dispersions of pea protein isolate (PPI), potato protein isolate (PoPI) and methylcellulose (MC) are shown in Fig. 1.

PPI displayed a main peak at ~20 μm, but also a smaller peak around 0.2 μm, indicating a coexistence of smaller protein aggregates and large protein agglomerates, although the small particles accounted only for ~0.1 % of total particle volume. The measured particle size distribution of PPI was consistent with values reported in literature (Janssen et al., 2024; Rivera del Rio et al., 2020; Sun et al., 2023). PoPI exhibited a monomodal size distribution, with a particle size of ~8 nm, reflecting the good dispersibility of the protein, in line with literature (Andlinger et al., 2022; Bahri et al., 2024; Baier & Knorr, 2015; Gelley et al., 2022). The average size of the MC samples was ~10 nm, irrespective of their molecular weight (M_w). This is slightly lower than reported previously, and could be attributed to the specific information obtained from light scattering compared to other methods (Kedzior et al., 2017). Nevertheless, the mentioned values provide an indication that the size of MC is similar to that of PoPI, and smaller than that of PPI.

Also the size distribution of MC-protein mixtures was investigated (data not shown). In all cases, the size distribution of all MC-protein mixtures was dominated by the protein, likely due to the higher scattering intensity of protein, masking the presence of MC molecules. For MC-PPI mixtures, the peak of the smaller protein particles at 0.2 μm was larger than for pure PPI, indicating that the degree of agglomeration was reduced. The incorporation of MC may have affected the degree of aggregation of PPI particles during mixing as it has been shown that high shear forces can disrupt non-covalent interactions (Janssen et al., 2024).

3.1.2. ζ-potential

The ζ-potentials of MC100, MC140, MC210 and MC300 were −0.8 ± 1.0, −0.4 ± 0.6, −0.5 ± 1.2 and 0.0 ± 0.4 mV, as expected for a non-

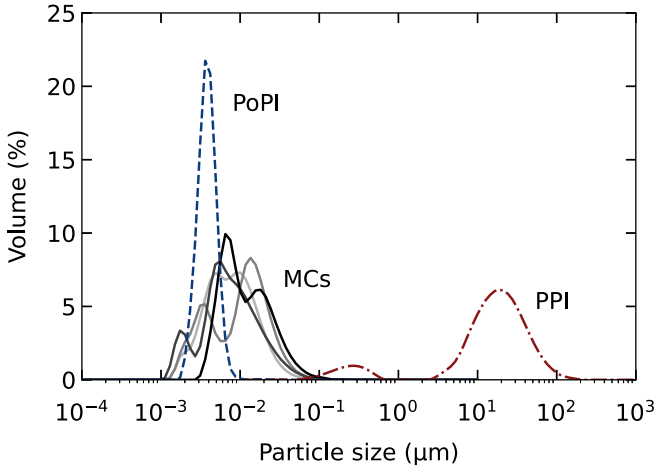

Fig. 1. Particle size distribution of pea protein isolate (PPI) as red dash-dotted line (-·-), potato protein isolate (PoPI) as blue dashed line (—), and the four methylcelluloses (MC) as solid lines (–) in greyscale. Increasing line darkness corresponds to increasing MC molecular weight (MC100, MC140, MC210 and MC300). Each distribution represents the average of three replicates.

ionic polymer (Kedzior et al., 2017; Ryu & McClements, 2024). PoPI and PPI exhibited ζ-potentials of −31.5 ± 3.8 and −30.8 ± 2.2 mV, respectively. Since the pH values of the PoPI and PPI samples were 6.6 and 6.2, respectively, both were above the isoelectric point of the proteins (PoPI: 4.5–5.2 (Gelley et al., 2022; Pots et al., 1999); PPI: 4.5–5.0 (Guldiken et al., 2023; Krishina et al., 1979)). As a result, both proteins carried a negative charge, which was consistent with expectations. These results are indicative of electrostatic repulsion between protein molecules, and no attractive electrostatic interactions were expected between MC and protein in these samples. The ζ-potential of MC-protein mixtures closely resembled those of protein alone, which was expected given that methylcellulose is uncharged and therefore did not contribute to the measured potential.

3.1.3. Thermal properties

The thermal properties of MC, proteins and their mixtures were examined using DSC to investigate the impact of protein type and concentration on MC gelation behaviour. Fig. 2 presents the onset (T_{onset}) and peak temperatures (T_{peak}) during heating for MC-PPI and MC-PPI mixtures as a function of protein concentration.

During heating of MC solutions, T_{onset} and T_{peak} ranged from 58.9 to 60.1 °C and 64.2–64.7 °C, showing that fibrillisation and subsequent assembly into a three-dimensional gel network occurred at the same temperature for all MCs. PoPI had a T_{onset} and T_{peak} of 58.7 °C and 65.8 °C, in line with values reported in literature (Andlinger et al., 2022; Gelley et al., 2022). Upon cooling, no enthalpy changes were observed, indicating the denaturation process of PoPI was irreversible. No enthalpy changes for the pea protein were detected at any of the tested concentrations (≤15 wt%). This confirmed the pea proteins in this isolate were already fully denatured prior to use, likely due to harsh extraction conditions. The full denaturation could partly be responsible for the large degree of PPI agglomeration. Significant main effects of both MC molecular weight and protein concentration on T_{onset} were observed, without any significant interaction effects. For T_{peak}, significant main effects of MC molecular weight, protein type, and protein concentration were observed, as well as significant interaction effects between all parameters. For example, the significant interaction between protein type and protein concentration indicates that the influence of protein concentration depended on the type of protein used. Full statistical details are provided in Table A1 in the Appendix.

The addition of PPI to MC solutions lowered T_{onset} and T_{peak} of MC gelation, without systematic effects of MC molecular weight. Since PPI did not contribute to the thermal transitions, MC must have been responsible for this shift. We suggest that PPI absorbed water, increasing the effective concentration of MC, making it easier to form fibrils and assemble into a network, which then occurred already at lower temperatures. This hypothesis was confirmed by the decrease in T_{onset} observed by increasing the concentration of MC (data not shown). Also the presence of PoPI influenced the T_{onset} of the mixtures. MC-PoPI mixtures had a lower T_{onset} than both the single-component MC and PoPI systems, which can again be explained by an increase in the effective concentration of both components. These results are in line with previous research by Ryu and McClements (2024). The peak temperature did not depend on PoPI concentration or MC molecular weight, but was similar to the T_{peak} values of pure PoPI. This showed that PoPI dominated T_{peak} of the gelation of the mixtures, suggesting that its denaturation temperature was not affected by the presence of MC. This also indicated that the decrease observed in T_{onset} with increasing PoPI concentration was solely caused by a higher effective MC concentration, and not by PoPI denaturing at lower temperatures. In none of the MC-PoPI mixtures, multiple peaks or shoulder peaks were observed, indicating that in these systems MC gelation and PoPI denaturation always occurred at the same temperature, in line with previous work (Ryu & McClements, 2024).

The DSC results suggested that the temperatures associated with gel network formation depended on the composition of the mixtures. To gain more insights into these effects, also the enthalpy change (ΔH) during these transitions was examined. Fig. 3 shows the enthalpy change of MC-protein mixtures and pure PoPI systems during heating. Significant main effects of MC molecular weight, protein type, and protein concentration on ΔH were observed, as well as significant interaction effects between all parameters (Table A1, Appendix). The endothermic enthalpy changes corresponding to the transition of pure MC systems were similar for MC140, MC210 and MC300 (~8.0 J/g), but such change was lower for MC100 (4.6 J/g), suggesting that gelation of MC100 required the least energy. This could potentially be a result of shorter MC fibrils and a less connected fibrillar network for MC100 compared to that of the other MCs in the study. This dependence of MC fibril length and network connectivity on molecular weight has been reported before by Schmidt et al. (2018). The addition of PPI (Fig. 3A) did not impact ΔH corresponding to MC gelation for MC100, while ΔH decreased with increasing PPI concentration for MC140, MC210 and MC300. This limited effect for MC100 could be related to the lower connectivity of the MC100 gel compared to that of the other MCs. Possibly, PPI could be included in the less connected, less dense MC network, without any hindrance. For MCs with higher M_w, the more interconnected networks were disturbed by the inclusion of PPI, allowing less connections between fibrils to be formed, leading to a

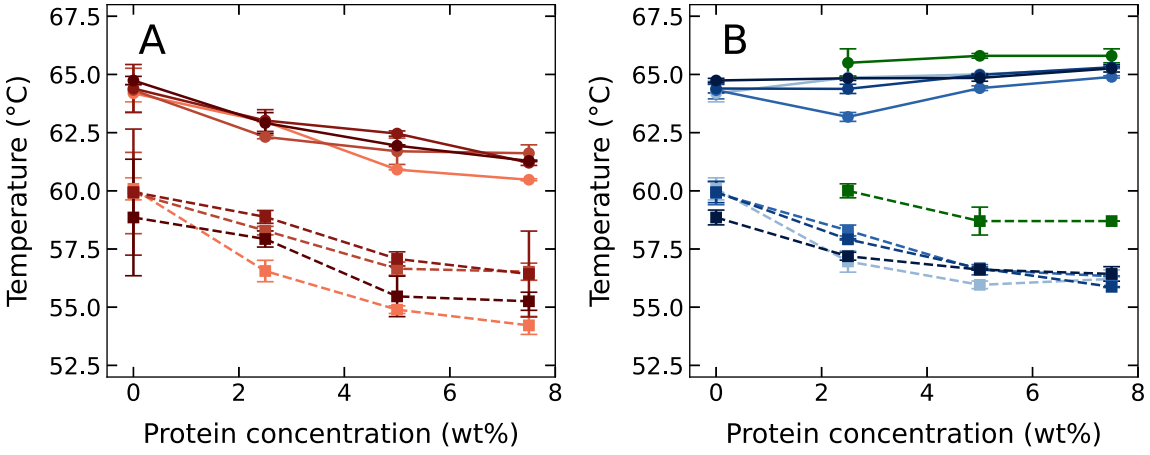

Fig. 2. Onset temperature (T_{onset}) as dashed (—) lines and peak temperature (T_{peak}) as solid (–) lines during heating for mixtures of methylcellulose (MC) and (**A**) pea protein isolate (PPI, red) and (**B**) potato protein isolate (PoPI, blue) as a function of protein concentration. Increasing line darkness corresponds to increasing MC molecular weight MC100, MC140, MC210 and MC300). All mixtures contained 2 wt% MC. The green dashed (—) and solid lines (–) in figure **B** represent T_{onset} and T_{peak} of pure PoPI samples, respectively. Error bars represent the standard deviation.

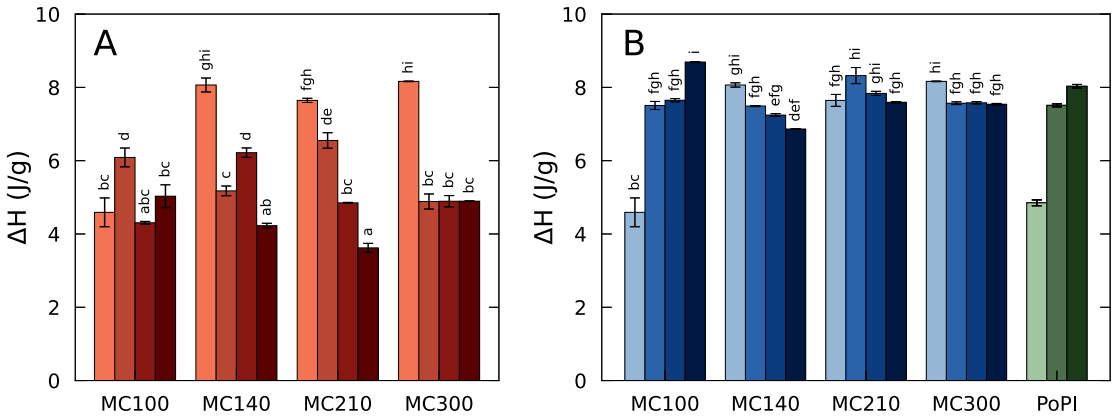

Fig. 3. Endothermic enthalpy change (ΔH) during heating for mixtures of methylcellulose (MC) in combination with (**A**) pea protein isolate (PPI, red) and (**B**) potato protein isolate (PoPI, blue) for the different MCs (MC100, MC140, MC210 and MC300), and data for PoPI (green). Increasing bar darkness corresponds to increasing protein concentration (0, 2.5, 5 and 7.5 wt%). Error bars represent the standard deviation and different letters indicate a significant difference in ΔH among different samples ($p < 0.05$).

lower ΔH.

For the MC-PoPI system (Fig. 3B), the results showed a different trend. Single-component systems of MC100 (4.6 J/g) and 2.5 % PoPI (4.8 J/g) had the lowest ΔH, while all other MC, PoPI and MC-PoPI systems generally had comparable ΔH values of around 7–8 J/g. For pure PoPI systems, higher protein concentrations resulted in a higher ΔH (ranging from 4.8 to 8.0 J/g), suggesting that more interactions occurred among proteins at higher concentrations. It can be stated that the mixture of MC100 and 2.5 % PoPI had a higher ΔH than expected based on ΔH of the individual ingredients. This was likely caused by the formation of more connections within the MC network, and within the PoPI network, as a result of an increased effective concentration of both MC and PoPI. At higher PoPI concentrations, MC100 samples had ΔH values similar to PoPI, indicating PoPI dominated gelation. In contrast, for samples of MC140, MC210 and MC300 with 2.5 % PoPI, the ΔH was similar to the one of the pure MC, suggesting MC dominated the thermal transition here. At PoPI concentrations of 5 and 7.5 %, MC-PoPI mixtures had comparable ΔH values to the single-component systems of MC and PoPI. Therefore, it cannot be concluded which ingredient dominated ΔH in these mixtures. Nevertheless, the fact that MC-PoPI mixtures displayed similar ΔH values as the individual systems suggests that MC and PoPI did not affect their thermal transitions, as was previously indicated by T_{onset} and T_{peak}.

In summary, DSC results showed that MC100 likely formed a less interconnected fibrillar network than MCs with higher M_w. Inclusion of PPI generally lowered the onset temperature of gelation and hindered formation of connections between MC fibrils. Similarly, the inclusion of PoPI lowered the temperature related to MC gelation, while the denaturation temperature of PoPI remained unaffected by MC. The implications of these thermal properties for gelation behaviour are discussed in detail from section 3.1.5 onwards.

3.1.4. *Shear viscosity*

The zero-shear viscosity (η_0) of MC-protein dispersions was determined from viscosity curves measured as a function of shear rate using the Carreau-Yasuda model (Equation (1)) and is shown in Fig. 4. The viscosities of 2 wt% MC100, MC140, MC210 and MC300 solutions at 20 °C, in the absence of protein, were 93, 388, 1176 and 4626 mPa s, respectively, which closely aligned with the supplier specifications. Significant main effects of MC molecular weight, protein type, and protein concentration on η_0 were observed, as well as significant interaction effects between all parameters, indicating that variations in one parameter can alter or amplify the effects of the others on viscosity (Table A1, Appendix).

For MC-PPI mixtures (Fig. 4A), viscosity increased with higher PPI concentrations across all MCs. This viscosity increase can be attributed to the combined effects of (a) a higher dry matter content in the solutions with PPI and (b) an increased effective concentration of MC due to

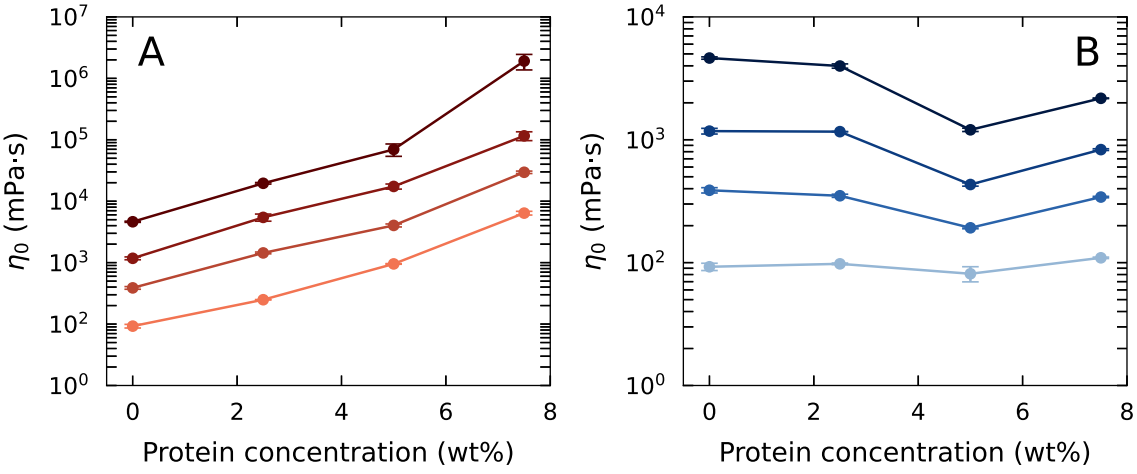

Fig. 4. Zero-shear viscosity (η_0) of methylcellulose-protein mixtures at 20 °C as a function of protein concentration for (**A**) pea and (**B**) potato protein isolate (PPI and PoPI) and the four different methylcellulose types. Increasing line darkness corresponds to increasing MC molecular weight (MC100, MC140, MC210 and MC300). All samples contained 2 wt% MC. Error bars represent the standard deviation of each data point.

water absorption by PPI. For MC-PoPI mixtures (Fig. 4B), the addition of the protein (up to 5 %) decreased the viscosity of MC solutions, which was more pronounced for MC with higher M_w. This reduction in viscosity suggests interactions between the two components, potentially leading to complexation between them. This complexation could reduce the amount of MC available for thickening. These interactions were likely of hydrophobic nature, since electrostatic interactions could be ruled out. The importance of hydrophobic interactions between MC and soy proteins has already been discussed by He et al. (2022). The small and comparable particle sizes of MC (~10 nm) and PoPI (~8 nm) may have facilitated closer molecular contact, enabling interactions between these two components. In contrast, the much larger size of PPI (~20 μm) provided a considerably lower surface area, limiting the ability of PPI to interact with MC. It is worth mentioning that these interactions between MC and PoPI did not impact the denaturation temperature of PoPI, as was discussed earlier. When PoPI concentration increased to 7.5 wt%, viscosity increased again, possibly because of electrostatic repulsion between the negatively-charged MC-PoPI complexes due to PoPI incorporation. Simultaneously, in samples with increasing PoPI concentration the dry matter content increased, potentially contributing to the increase in viscosity.

In summary, PPI did not show any direct interactions with MC, whereas PoPI affected the network by formation through hydrophobic interactions with MC. These differences in interactions could be expected to impact the microstructure and mechanical properties of the different MC-protein gels.

3.1.5. Gelation behaviour

MC is known to form a space-spanning gel network upon heating. The gelation behaviour of the MCs, and both PPI and PoPI, was measured using small amplitude oscillatory shear experiments. The storage modulus (G′) of these samples as a function of temperature is shown in Fig. 5. All MC solutions exhibited thermo-reversible gelation. This behaviour is briefly discussed to provide context before investigating the MC-protein mixtures.

At 20 °C, G′ of the MC solutions was related to their viscosity, with MC100 having the lowest G′ and MC300 the highest. Upon heating to 60 °C, G′ increased gradually, likely due to enhanced hydrophobic interactions between MC chains, but the values remained too low (<50 Pa) to indicate gelation. When the temperature exceeded 60 °C, G′ increased sharply, driven by the fibrillisation of MC and the subsequent formation of a fibrillar network. This gelation temperature was similar to the onset of gelation found in DSC measurements (Fig. 2) and aligns with values commonly reported in the literature (McAllister, Lott et al., 2015; Schmidt et al., 2018). At 70 °C, the gel strength plateaued, with the MC100 gel exhibiting a lower G′ (1408 Pa) than the gels of MC140, MC210 and MC300 (1833, 1873, 1894 Pa). This difference was likely due to the formation of shorter fibrils and a less connected gel network for MC100, as supported by Schmidt et al. (2018). This was also in agreement with DSC measurements, where MC100 showed the lowest ΔH during heating (Fig. 3). During cooling, the temperature of dissolution was observed to range between 30 and 50 °C, illustrating the hysteresis in MC gelation.

The 2.5 % PoPI solution did not gel during the temperature sweep, while the 5 % and 7.5 % solutions did. At these higher concentrations, G′ increased with temperature and continued to increase during cooling. This behaviour is typical of protein gelation, driven by protein denaturation, inducing hydrophobic interactions at elevated temperatures. Contribution of disulfide bonds to potato protein gelation was negligible as the main potato protein, patatin, only contains one free thiol group, which does not allow for the formation of an interconnected network via S-S bonds (Tanger et al., 2021a, 2021b). As the system cooled down, hydrophobic interactions decline, but hydrogen bonding further strengthened the gel network, as previously reported by other researchers (Tanger, Andlinger, et al., 2021). Higher PoPI concentrations resulted in higher G′ values due to increased protein interactions within the network. In contrast, PPI dispersions did not form gels, as indicated by the flat G′ curve for the 10 % PPI sample in Fig. 5B. This lack of gelation was attributed to the high denaturation and aggregation level of the protein prior to use, leading to the loss of key structural and functional properties.

3.2. Microstructure of MC-protein gels

Before discussing the mechanical properties and syneresis behaviour of MC-protein gels, we first discuss their microstructural characteristics. The microstructure of the MC-protein gels was investigated using confocal laser scanning microscopy (CLSM). Images were taken at 70 °C to characterise the gel structure formed upon heating. Additional images were taken before and after heating (both at 20 °C), but these are not shown. Fig. 6A shows the microstructure of MC-PPI mixtures ranging from 0 % protein (pure MC) to 7.5 wt% PPI at 70 °C. For a quantitative comparison of the images, the volume fraction (ϕ), diameter and connectivity of the MC- and PPI-rich domains were determined using image analysis.

In the absence of PPI, a fine homogeneous MC-network was visible,

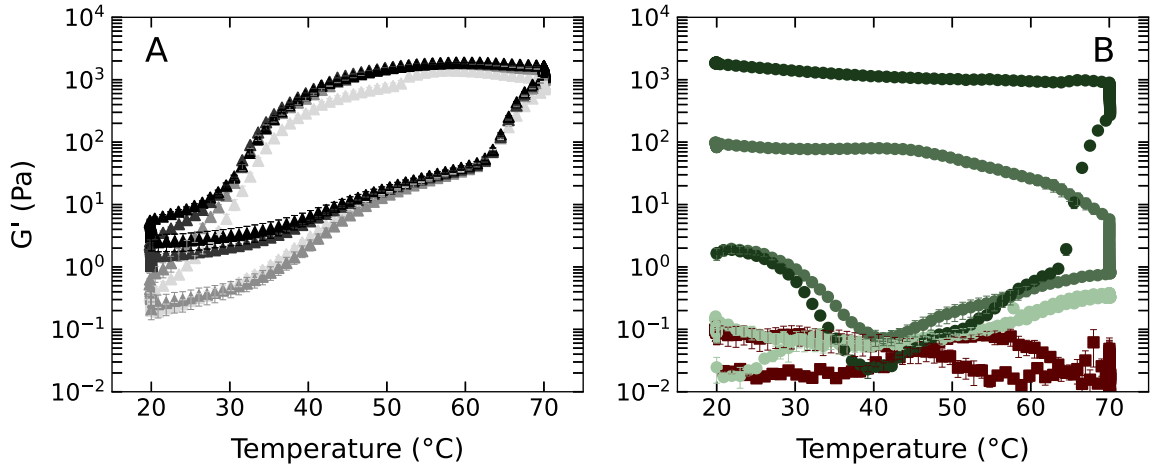

Fig. 5. Storage modulus (G′) of (**A**) the four methylcelluloses (MC) and (**B**) pea protein isolate (PPI, red squares) and potato protein isolate (PoPI, green spheres) solutions as a function of temperature. The samples of figure **A** all contained 2 wt% MC. Increasing symbol darkness corresponds to increasing MC molecular weight (MC100, MC140, MC210 and MC300). In figure **B,** the red squares represent a 10 wt% PPI dispersion, and the green spheres represent PoPI samples. Increasing symbol darkness corresponds to increasing PoPI concentration (2.5, 5 and 7.5 wt%). Error bars represent the standard deviation.

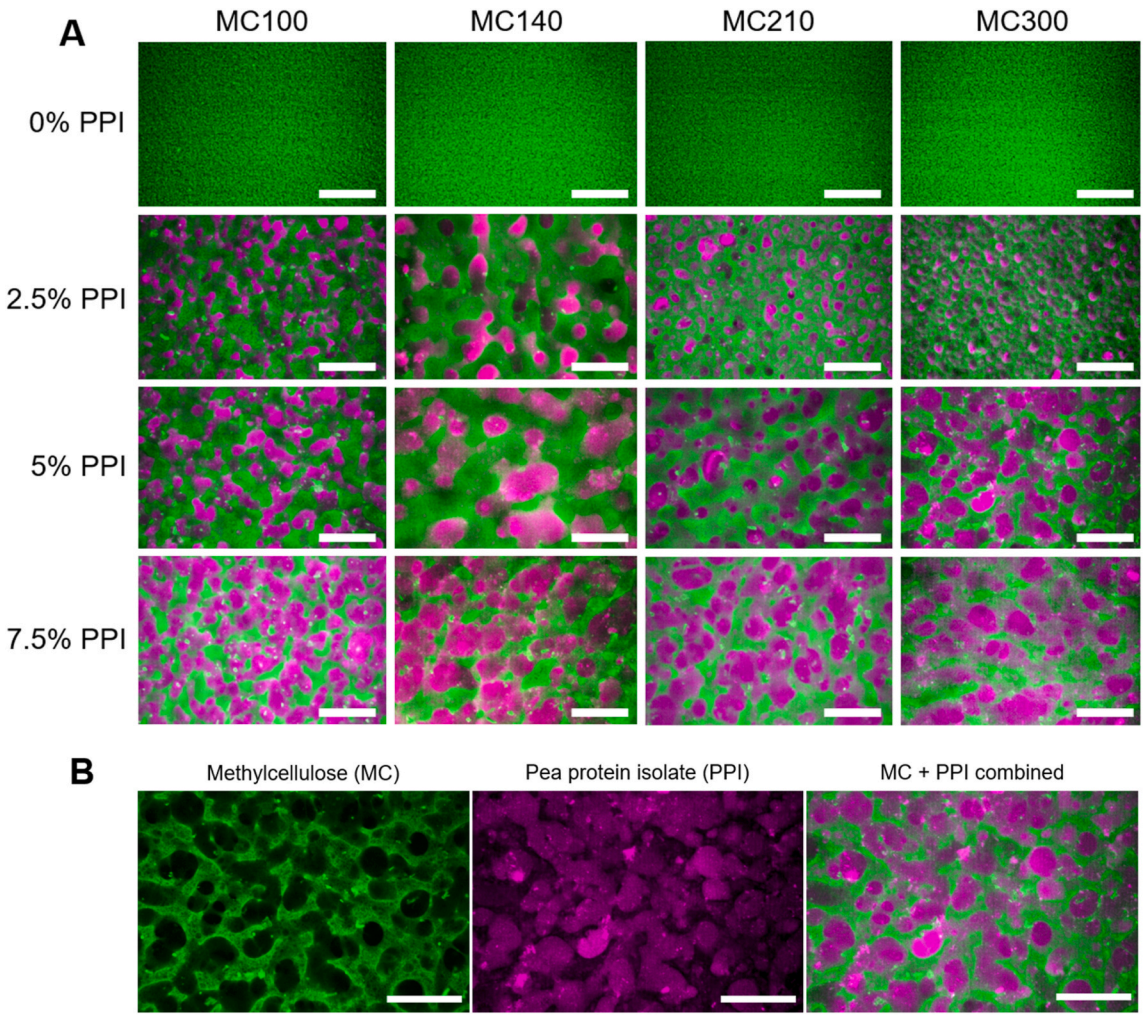

Fig. 6. (**A**) Confocal laser scanning microscopy (CLSM) images of gels containing methylcellulose (MC) and pea protein isolate (PPI) at 70 °C. Rows show increasing PPI concentrations (0, 2.5, 5 and 7.5 wt%), and columns the MC type (MC100, MC140, MC210 and MC300). (**B**) Example CLSM images of a mixture of 2 wt% M300 and 5 wt% PPI at 70 °C. The left and middle images display individual channels for MC and PPI, while the right image shows their overlay. In all images, magenta indicates PPI-rich domains and green indicates MC-rich domains. The scale bar represents 100 μm.

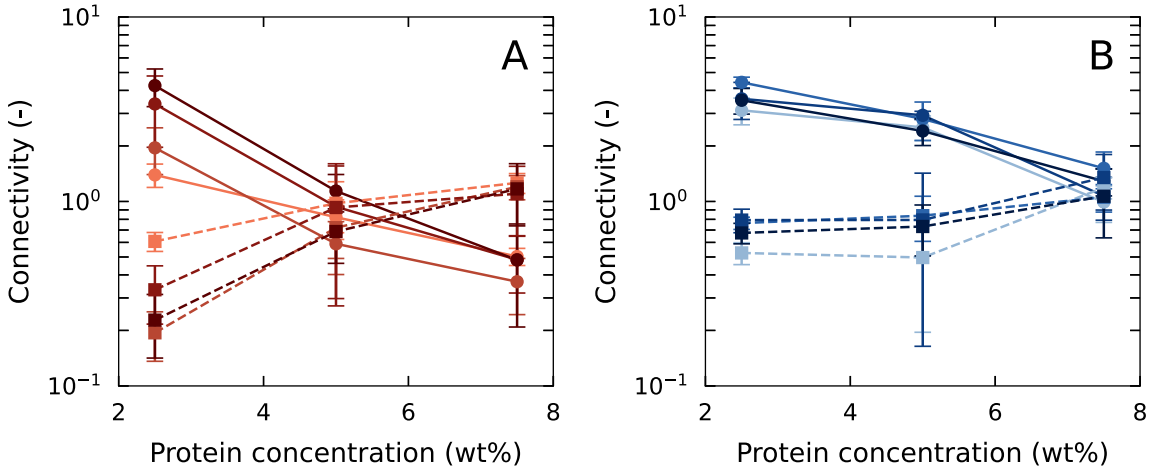

Fig. 7. Connectivity of methylcellulose-rich domains (solid lines) and protein-rich domains (dashed lines) of methylcellulose-protein mixtures containing (**A**) pea protein isolate (PPI) and (**B**) potato protein isolate (PoPI) at 70 °C. Increasing line darkness corresponds to increasing MC molecular weight (MC100, MC140, MC210 and MC300). All samples contain 2 wt% MC. Error bars represent the standard deviation.

with a pore size and MC network thickness of ~2 μm (Fig. S3, Supplementary material B). Before heating and after cooling, this network was not visible, indicative of the thermo-reversibility of MC gelation. A clear separation between PPI-rich and MC-rich domains could be observed in all samples. The volume fraction of these domains was independent of MC molecular weight, and was solely determined by PPI concentration. Samples with 2.5, 5 and 7.5 % PPI had MC volume fractions (ϕ_{MC}) of ~0.64, 0.48 and 0.33, showing that ϕ_{MC} decreased proportionally with increasing PPI concentration. This affected the effective concentrations of MC and PPI in these samples, driven by the specific water holding capacity of the ingredients, and the water distribution between MC and PPI domains. PPI-rich domains also increased in size with increasing PPI concentration (2.5–7.5 %), while the MC-rich domains remained relatively constant in size (Fig. S3, Supplementary material B). This was expected, as the added PPI favoured further agglomeration, contributing to the enlarged PPI-rich domains. The observation that MC-domain size remained unaffected suggested that it formed a more stable percolating network resisting coarsening. Besides domain size, also the connectivity of the MC- and PPI-rich domains were determined and represented in Fig. 7.

Significant main effects of MC molecular weight, protein type, and protein concentration on the connectivity of the protein-rich domains were observed, as well as significant interaction effects between all parameters (Table A1, Appendix). For the connectivity of the MC-rich domains, only significant main effects of MC molecular weight and protein concentration were observed, with interactions only between MC molecular weight and protein type, and protein type and protein concentration. PPI inclusion into MC gels resulted in a decreasing connectivity of MC domains and an increasing connectivity of PPI domains. At low PPI concentration (2.5 %), the connectivity of the MC-rich domains increased with M_w of MC, while PPI-connectivity decreased. This was likely due to the higher viscosity of the MC phase at increased M_w, which slowed down PPI diffusion. The resulting reduction in mobility may have delayed the early formation of separated PPI-rich domains, allowing a more connected network to form. The effect of MC molecular weight became negligible at higher PPI concentrations, as there was sufficient PPI present to form large connected PPI domains. Despite the presence of such domains, MC still formed an interconnected network, although to a lesser extent than PPI. Addition of PPI therefore hindered the formation of connections between MC, but did not completely prevent it. This was also confirmed by the fine network visible in MC gels (Fig. 6A), which persisted within the MC-domains of MC-PPI mixtures, as better visualised in Fig. 6B. Besides the fine MC network, the individual CLSM channels for MC (left) and PPI (middle) show a clear separation in domains, in which PPI domains are enclosed in a MC continuous network. The more detailed images of the separate channels were also important for quantitative analysis, as the combined images could not capture these important microstructural features. All the

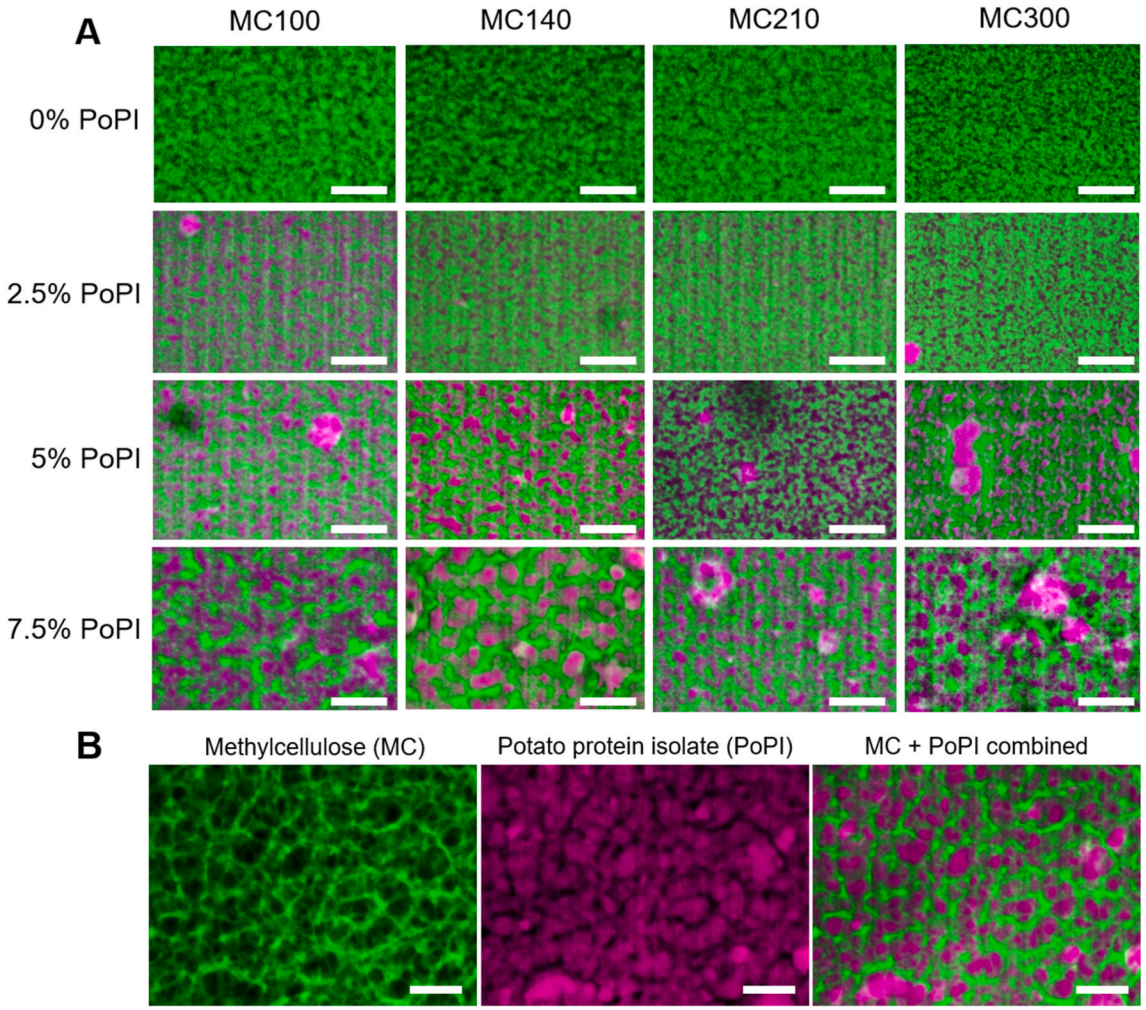

Fig. 8. (**A**) Confocal laser scanning microscopy images of gels containing methylcellulose (MC) and potato protein isolate (PoPI) at 70 °C. Rows correspond to PoPI concentrations of 0, 2.5, 5 and 7.5 wt%, and columns correspond to the MC type (MC100, MC140, MC210 and MC300). (**B**) Example CLSM images of a mixture of 2 wt% MC140 and 7.5 wt% PoPI at 70 °C. The left and middle images display individual channels for MC and PoPI, while the right image shows their overlay. In all images, magenta indicates PoPI-rich domains and green indicates MC-rich domains. The scale bar represents 25 μm.

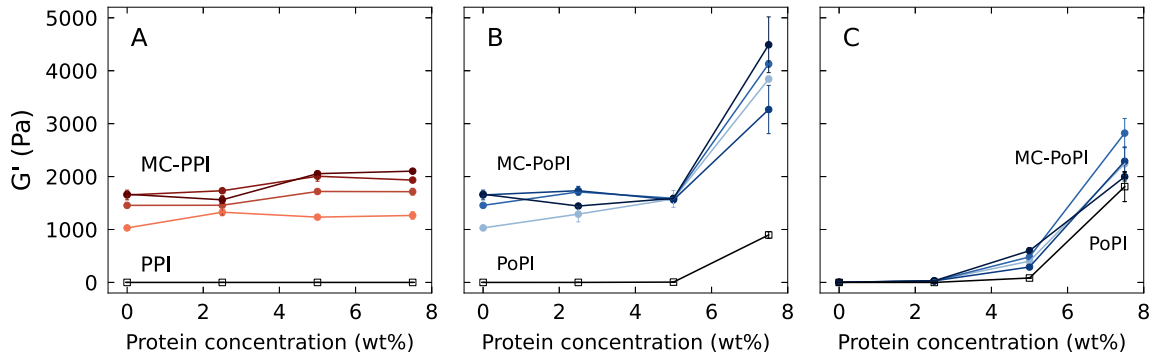

Fig. 9. Storage modulus (G′) of mixtures of methylcellulose-protein mixtures for (**A**) pea protein isolate (PPI) at 70 °C and potato protein isolate (PoPI) at (**B**) 70 °C and (**C**) 20 °C. Open black squares represent pure protein samples, and increasing line darkness for the filled spheres corresponds to increasing MC molecular weight (MC100, MC140, MC210 and MC300). All samples contained 2 wt% MC. Error bars represent the standard deviation.

observed differences in gel microstructures may impact functional properties, such as gel strength and syneresis.

Also the microstructure of MC-PoPI gels was visualised with CLSM (Fig. 8A). At 2.5 % PoPI, the microstructure of the MC gel remained largely intact, with PoPI distributed within the pores of the MC network. For MC with lower M_w, the gel structure became coarser, with larger MC- and PoPI-rich domains (Fig. S4, Supplementary material B), although this effect was relatively small. Nevertheless, this suggested that 2.5 % PoPI was sufficient to disrupt gels of MC with lower M_w. A lower M_w resulted in a less interconnected MC network, making it more susceptible to interference in network formation by PoPI. Increasing the PoPI concentration to 5 % did not lead to drastic further coarsening of the gel structure, but a decrease in the connectivity of the MC-domains was observed (Fig. 7B). At 7.5 % PoPI, the PoPI-domains became considerably larger and also began to interconnect for all MC molecular weights tested. In these 7.5 % PoPI samples, the connectivity of MC and PoPI domains became comparable, suggesting the formation of a bi-continuous gel network during heating. While the space-spanning MC network is visible in the CLSM images, the connections between the PoPI domains are less distinct. However, by examining the individual channels for MC and PoPI separately (Fig. 8B), it became evident that the PoPI domains also formed a space-spanning network. Such a bi-continuous structure has not yet been reported in literature. One study reported the microstructure of MC-PoPI gels, but these gels showed an MC-continuous gel with large PoPI inclusions (Ryu & McClements, 2024). However, in the mentioned study, the gel microstructure was measured at 20 °C instead of an elevated temperature at which MC is also able to form a gel.

While the domain size (Figure S3 and Figure S4, Supplementary material B) was dependent on the M_w of MC, the volume fractions of these domains did not vary across samples with different MC, and were solely determined by PoPI concentration, in a similar way as for PPI. Samples with 2.5, 5 and 7.5 % PoPI had a ϕ_{MC} of around 0.68, 0.62 and 0.49, respectively. In conclusion, analysis of gel microstructures revealed phase separation in MC-PPI gels and the structural shift in MC-PoPI gels towards bi-continuous networks at higher PoPI concentrations. These differences in structural organisation are likely to have a substantial impact on the syneresis and mechanical properties of these gels. Notably, to the best of our knowledge, this study is the first to report MC–protein microstructures at elevated temperatures that are relevant for applications like meat analogues, providing new insights into their functional behaviour under such conditions.

3.3. Mechanical properties and syneresis of MC-protein gels

Based on the large variation in the microstructure of MC-protein gels, we expected that the functional properties of the gels depended on the specific combination of ingredients. The following sections include the mechanical properties and syneresis behaviour, with a discussion on the link between these properties and the microstructure.

3.3.1. Viscoelastic properties

The storage modulus (G′) of all MC-protein gels was determined as a function of protein concentration (Fig. 9). For PPI, only G′ at 70 °C is shown, as the gels melted upon cooling to 20 °C, and PPI was not able to form a protein network. As PoPI was able to form a protein network, G′ values both at 70 °C and after cooling to 20 °C are presented. With increasing PPI concentration (Fig. 9A), G′ remained relatively stable. This indicated that the disruption of the MC gel as observed in CLSM images (Fig. 6) and the resulting decrease in the connectivity of MC-rich domains (Fig. 7A) did not weaken the gels. Weakening was likely counteracted by the densification of the MC network, as PPI absorbed part of the water within the systems. For MC-PoPI gels, an effect of protein concentration was seen both at 70 °C and 20 °C. At 70 °C, the G′ of MC-PoPI gels was similar to that of pure MC gels up to a PoPI concentration of 5 %, suggesting that MC predominated in these systems, and likely formed a continuous gel network. This is consistent with the microstructure of these gels (Fig. 8) and the high connectivity of the MC-rich domains and low connectivity of PoPI-rich domains (Fig. 7B). PoPI acted as a dispersed phase without altering G′. Only the relatively weak MC100 gel, compared to the other MC gels, was strengthened at PoPI concentrations below 5 %. This aligned with CLSM images of MC100 gels, in which PoPI addition induced the most pronounced structural changes. When the PoPI concentration increased to 7.5 %, a steep increase in G′ was observed, reflecting a major change in gel behaviour. This sharp increase suggested that PoPI began to form its own space-spanning network, altering the overall gel structure. This is supported by CLSM images that revealed coarsening of the gel network, while the connectivity of the PoPI-rich domains increased and became similar to that of MC. These results thus confirmed the formation of a bi-continuous network. Interestingly, the G′ of the MC-PoPI gels at 70 °C were higher (~3300–4500 Pa) than the sum of the G′ of MC (~1000–1700 Pa) and PoPI gels (900 Pa), suggesting a synergistic effect during the co-gelation of MC and PoPI. This could be due to the increased effective concentrations of both MC and PoPI, yielding firmer gels than the individual systems. Additionally, hydrophobic interactions between MC and PoPI may create a coupled gel network, strengthening

the overall system.

When MC-PoPI gels were cooled to 20 °C, G′ decreased for the different samples, suggesting that the MC gel had melted and the PoPI network determined the gel modulus. The cooled MC-PoPI samples were always stronger than pure PoPI samples. This may be attributed to an increased effective PoPI concentration in the presence of MC during gelation, which influenced the resulting structure and the corresponding G′. In addition, the hydrophobic interactions between MC and PoPI during gelation may have altered the network structure, although these interactions reduced again during cooling. Our results were in contrast with the findings of Ryu and McClements (2024), who reported weaker gels, attributed to an interference of PoPI gel formation by the presence of MC. However, in their study they used a different MC to PoPI ratio and MC specifications were not disclosed, making direct comparisons challenging. Moreover, the reported ζ-potential of their MC was −13.2 mV, which is unusual for a neutral polymer like MC. This could indicate impurities in their system or a MC type with very different properties, potentially causing an interference with PoPI gel formation. This may explain the discrepancy with the results of our samples.

3.3.2. Textural properties

Next to G′, also the nominal indentation stress of MC-protein gels was evaluated using a displacement-controlled indentation test. Fig. 10 shows the nominal indentation stress of MC-PPI and MC-PoPI gels at 70 °C. Significant main effects of MC molecular weight, protein type, and protein concentration on the nominal indentation stress were observed, as well as significant interaction effects between MC molecular weight and protein type, MC molecular weight and protein concentration, and protein type and concentration (Table A1, Appendix).

The addition of PPI to MC gels (Fig. 10A) did not affect the nominal indentation stress, similar to its impact on G′. In line with results obtained for small deformations, the stress of MC100 samples was lower than those with the other MCs. For MC-PoPI samples (Fig. 10B), the nominal indentation stress increased proportionally with PoPI concentration. Interestingly, this trend differed from the results shown before (Fig. 9), where G′ increased only at 7.5 % PoPI. This discrepancy was probably related to the differences in the type and scale of deformation applied. Small amplitude oscillatory deformations probe the linear viscoelastic properties of gels without disturbing their overall structure. In contrast, large deformations involve applying strains large enough to alter or break the gel network, thereby testing the bulk mechanical properties of the gel. As a result, small deformation measurements are sensitive to the connectivity and structure of the network, and are not considerably affected by individual particles or dispersed domains. At low PoPI concentrations (≤5 %), the gel structure was dominated by a continuous MC network, while at higher PoPI concentrations, the structure transitioned to a bi-continuous gel. This marked structural change altered the G′ measured under small deformations. Under large deformations, the inclusion of PoPI domains, whether connected or not, provided additional structural integrity to the material, making it more resistant to compressive forces during indentation.

3.3.3. Syneresis during gelation

MC gels are known to exhibit syneresis during gelation, which was also observed in our experiments. No data for MC-PoPI gels are shown, as these samples did not display any syneresis. As concluded from the microstructure and mechanical properties of the gels, potato proteins formed a network that effectively retained water, preventing its release during gelation in mixtures with MC. This finding was in contrast with findings of Ryu and McClements (2024), who reported around 2 % syneresis for MC-PoPI gels. This was likely attributed to a higher MC molecular weight in their study. On the other hand, gels with PPI did show syneresis (Fig. 11), due to the lack of a gelled PPI protein network.

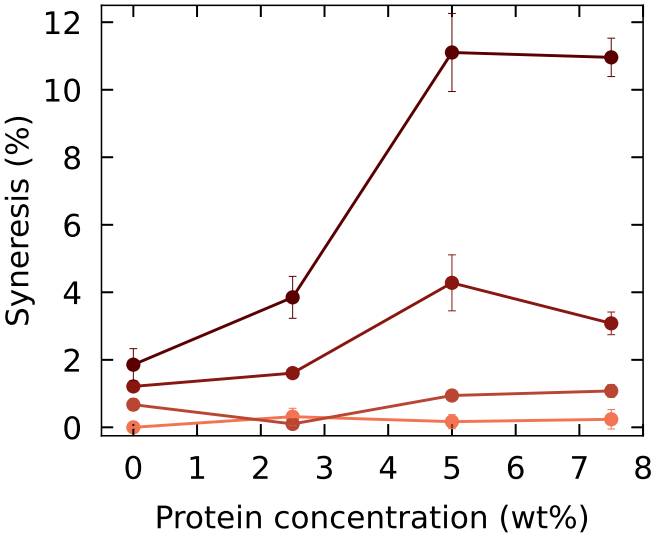

Fig. 11. Syneresis of mixtures of methylcellulose (MC) and pea protein isolate (PPI) during gelation. Increasing line darkness corresponds to increasing MC molecular weight (MC100, MC140, MC210 and MC300). All samples contained 2 wt% MC. Error bars represent the standard deviation.

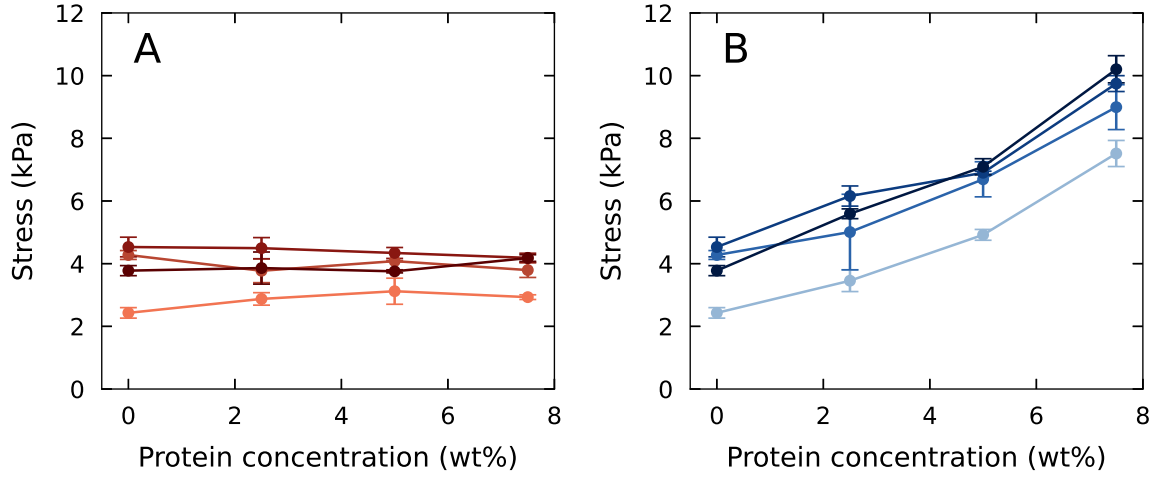

Fig. 10. Nominal indentation stress of methylcellulose-protein mixtures for (**A**) pea protein isolate (PPI) and (**B**) potato protein isolate (PoPI) at 70 °C. Increasing line darkness corresponds to increasing MC molecular weight (MC100, MC140, MC210 and MC300). All samples contained 2 wt% MC. Error bars represent the standard deviation.

Significant main effects of MC molecular weight and PPI concentration on the nominal indentation stress were observed, as well as a significant interaction effects between these two parameters (Table A2, Appendix).

MC samples without protein exhibited syneresis between 0 and 2 %, with higher M_w leading to more syneresis. The addition of PPI influenced syneresis, but depended on the M_w of MC. MC100 and MC140 showed minimal syneresis in pure MC systems and were unaffected by the presence of PPI. In contrast, MC210 and MC300 displayed increased syneresis with higher PPI concentrations. As MC forms a network on its own, it is mostly likely that in our samples the liquid was released from the PPI-domains. To gain more insight into syneresis, the dry matter and particle size of the expelled liquid were measured. For MC210 samples, the dry matter of the expelled liquid was 0.0 ± 0.0, 1.6 ± 0.2, 5.7 ± 0.1 and 8.3 ± 0.0 wt%, for 0, 2.5, 5 and 7.5 wt% PPI, respectively. For MC300 samples, the dry matter was 0.0 ± 0.0, 1.2 ± 0.2, 5.5 ± 0.3 and 8.5 ± 0.4 wt%. The dry matter was probably predominantly represented by protein. Therefore, the dry matter content of the expelled liquid was similar to the initial protein content of the mixtures. This indicated that the composition of the expelled liquid generally reflected the overall protein content of the gels, regardless of M_w.

For 5 and 7.5 % PPI, the dry matter content of the expelled liquid was higher than the initial protein content. This reflected the increased effective concentration in the PPI domains, due to the water absorption capacity of the MC gel. The particle size of the expelled liquid was ~0.5 μm, representing small PPI aggregates. The fact that only small particles were present in the expelled liquid suggested that larger agglomerates that were still present were not released, and small aggregates were concentrated to higher levels due to water absorption by MC. Particles larger than 0.5 μm were most likely retained in the gel network, unable to diffuse through the gel due to their large size. The exclusive release of small particles corroborated the gel microstructure, where we observed that the fine MC network (~2 μm) was present in all MC-PPI gels (Fig. 6). This network allowed the 0.5 μm to pass while blocking the larger particles. The increase in syneresis with higher PPI concentrations was attributed to larger and more interconnected PPI domains as observed in CLSM images. Since PPI could not form a gel, these domains were liquid and acted as channels for liquid to expel from the gel. Syneresis could therefore be triggered by the inclusion of proteins that did not form a gel by themselves, but induced phase separation instead.

4. Conclusions

This study examined the effects of methylcellulose (MC) molecular weight and protein characteristics on the structural and mechanical properties of MC-protein gels. By systematically varying MC molecular weight and employing two distinct protein isolates—potato protein isolate (PoPI) with high nativity and solubility, and pea protein isolate (PPI) with a high degree of denaturation and aggregation—we gained insights into the gelation behaviour of MC-protein mixtures.

We demonstrated that protein characteristics strongly affect gel microstructure, water retention and mechanical strength. In MC-PPI gels, increasing PPI concentration resulted in the formation of large and interconnected protein-rich domains that significantly enhanced syneresis, especially in gels with high-molecular weight MC. These microstructural changes did not impact gel strength of MC-PPI gels. In the case of PoPI, with better gelling ability than PPI, proteins formed the dispersed phase within MC gels at low proteins concentration. The ability of PoPI to form a gel and the high water-holding capacity of the PoPI network completely prevented syneresis. When the PoPI concentration was sufficiently high, PoPI formed a three dimensional network alongside MC, leading to a synergistic increase in gel strength. This enhanced strength was attributed to increased effective concentrations of both MC and PoPI, along with the probable formation of a coupled gel network through hydrophobic interactions between MC and PoPI.

These findings indicate that the interplay between protein characteristics and MC molecular weight allows for control over gel properties such as texture and water binding, properties highly relevant for food applications such as meat analogues, where texture and juiciness are key. Future research should investigate more subtle changes in protein characteristics along the spectrum, next to the two extremes studied here. Overall, these findings contribute to a better understanding of the microstructure and functional properties of MC-protein gels, and can help with the design of plant-based food gels with tailored functional properties.

CRediT authorship contribution statement

Thiemo van Esbroeck: Writing – original draft, Visualization, Validation, Methodology, Investigation, Data curation, Conceptualization. **Guido Sala:** Writing – review & editing, Validation, Supervision, Conceptualization. **Markus Stieger:** Writing – review & editing, Validation, Supervision, Funding acquisition, Conceptualization. **Elke Scholten:** Writing – review & editing, Validation, Supervision, Funding acquisition, Conceptualization.

Declaration of generative AI and AI-assisted technologies in the writing process

During the preparation of this work, the authors used ChatGPT (OpenAI) and Google Gemini to improve readability and language. After using these tools, the authors reviewed and edited the content as needed and take full responsibility for the content of the publication.

Declaration of competing interest

The authors declare that they have no known competing financial interests or personal relationships that could have appeared to influence the work reported in this paper.

Acknowledgements

This research was performed within the framework of the public-private partnership project “Improving sensory quality of meat analogues” funded by the Topsector Agri & Food (TKI, grant number LWV-20.078, the Netherlands). The authors would like to thank Kiriakos Krimniotis for his valuable contributions to the preliminary experiments.

Appendix A. Supplementary data

Supplementary data to this article can be found online at https://doi.org/10.1016/j.foodhyd.2025.112189.

Appendix

Table A1
F and *p* values (NS $p > 0.05$, *$p < 0.05$, **$p < 0.01$, ***$p < 0.001$) derived from three-way MANOVA with MC molecular weight, protein type, protein concentration and their interaction as fixed factors.

	MC		Protein		Protein concentration		MC x protein		MC x concentration		Protein x concentration		MC x protein x concentration	
	F(3,32)	*p*	F(1,32)	*p*	F(3,32)	*p*	F(3,32)	*p*	F(6,32)	*p*	F(2,32)	*p*	F(6,32)	*p*
Onset temperature (T_{onset})	5.2	**	0.7	NS	61.6	***	1.7	NS	1.0	NS	0.9	NS	0.5	NS
Peak temperature (T_{peak})	7.6	***	495.3	***	46.5	***	10.0	***	8.2	***	88.5	***	7.9	***
Enthalpy (ΔH)	38.4	***	1337.9	***	75.0	***	8.5	***	95.1	***	169.6	***	10.7	***
Viscosity (η_0)	26.2	***	32.2	***	27.9	***	25.6	***	23.0	***	28.0	***	23.0	***
Storage modulus 70 °C	34.7	***	199.7	***	330.9	***	9.5	***	6.1	***	242.5	***	4.8	***
Nominal indentation stress	93.5	***	587.6	***	130.4	***	8.9	***	4.2	**	135.8	***	1.4	NS
	F(3,102)	*p*	F(1,102)	*p*	F(3,102)	*p*	F(3,102)	*p*	F(6,102)	*p*	F(2,102)	*p*	F(6,102)	*p*
Connectivity MC-rich domains	4.3	**	1.5	NS	58.5	***	4.0	**	0.3	NS	6.8	**	1.3	NS
Connectivity protein-rich domains	6.4	***	243.2	***	247.1	***	14.8	***	7.6	***	11.2	***	6.4	***

Table A2
F and *p* values (NS $p > 0.05$, *$p < 0.05$, **$p < 0.01$, ***$p < 0.001$) derived from two-way ANOVA with MC molecular weight and protein concentration and their interaction as fixed factors.

	MC		Protein concentration		MC x concentration	
	F(3,32)	*p*	F(3,32)	*p*	F(6,32)	*p*
Storage modulus 20 °C *(MC-PoPI samples)*	4.3	**	58.5	***	0.3	NS
Syneresis *(MC-PPI samples)*	6.4	***	247.1	***	7.6	***

Data availability

Data will be made available on request.

References

Almeida, N., Rakesh, L., & Zhao, J. (2018). The effect of kappa carrageenan and salt on thermoreversible gelation of methylcellulose. *Polymer Bulletin, 75*, 4227–4243. https://doi.org/10.1007/s00289-017-2256-z

Andlinger, D. J., Schrempel, U., Hengst, C., & Kulozik, U. (2022). Heat-induced aggregation kinetics of potato protein – Investigated by chromatography, calorimetry, and light scattering. *Food Chemistry, 389*, Article 133114. https://doi.org/10.1016/J.FOODCHEM.2022.133114

Arvidson, S. A., Lott, J. R., McAllister, J. W., Zhang, J., Bates, F. S., Lodge, T. P., Sammler, R. L., Li, Y., & Brackhagen, M. (2013). Interplay of phase separation and thermoreversible gelation in aqueous methylcellulose solutions. *Macromolecules, 46*(1), 300–309. https://doi.org/10.1021/MA3019359

Bahri, A., Charpentier, C., Khati, P., Parc, R. Le, Chevalier-Lucia, D., & Picart-Palmade, L. (2024). Long-time high-pressure processing of a patatin-rich potato proteins isolate: Impact on aggregation and surface properties. *International Journal of Food Science and Technology*. https://doi.org/10.1111/IJFS.17192

Baier, A. K., & Knorr, D. (2015). Influence of high isostatic pressure on structural and functional characteristics of potato protein. *Food Research International, 77*, 753–761. https://doi.org/10.1016/J.FOODRES.2015.05.053

Bodvik, R., Dedinaite, A., Karlson, L., Bergström, M., Bäverbäck, P., Pedersen, J. S., Edwards, K., Karlsson, G., Varga, I., & Claesson, P. M. (2010). Aggregation and network formation of aqueous methylcellulose and hydroxypropylmethylcellulose solutions. *Colloids and Surfaces A: Physicochemical and Engineering Aspects, 354*(1–3), 162–171. https://doi.org/10.1016/J.COLSURFA.2009.09.040

Chatterjee, T., Nakatani, A. I., Adden, R., Brackhagen, M., Redwine, D., Shen, H., Li, Y., Wilson, T., & Sammler, R. L. (2012). Structure and properties of aqueous methylcellulose gels by small-angle neutron scattering. *Biomacromolecules, 13*(10), 3355–3369. https://doi.org/10.1021/BM301123A

Chen, C.-H., Tsai, C.-C., Chen, W., Mi, F.-L., Liang, H.-F., Chen, S.-C., & Sung, H.-W. (2006). Novel living cell sheet harvest system composed of thermoreversible methylcellulose hydrogels. *Biomacromolecules, 7*, 736–743. https://doi.org/10.1021/bm0506400

Coughlin, M. L., Liberman, L., Piril Ertem, S., Edmund, J., Bates, F. S., & Lodge, T. P. (2021). Methyl cellulose solutions and gels: Fibril formation and gelation properties. *Progress in Polymer Science, 112*, Article 101324. https://doi.org/10.1016/j.progpolymsci.2020.101324

Fairclough, J. P. A., Yu, H., Kelly, O., Ryan, A. J., Sammler, R. L., & Radler, M. (2012). Interplay between gelation and phase separation in aqueous solutions of methylcellulose and hydroxypropylmethylcellulose. *Langmuir, 28*(28), 10551–10557. https://doi.org/10.1016/j.progpolymsci.2020.101324

Gelley, S., Lankry, H., Glusac, J., & Fishman, A. (2022). Yeast-derived potato patatins: Biochemical and biophysical characterization. *Food Chemistry, 370*, Article 130984. https://doi.org/10.1016/J.FOODCHEM.2021.130984

Guldiken, B., Saffon, M., Nickerson, M. T., & Ghosh, S. (2023). Improving physical stability of pea protein-based emulsions near the isoelectric point via polysaccharide complexation. *Food Hydrocolloids, 145*, Article 109029. https://doi.org/10.1016/J.FOODHYD.2023.109029

He, J., Peng, Z., Yang, J., Dai, L., Hua, Z., & Li, L. (2022). How does soy 7S globulin influence the thermo-responsive fibration process of methylcellulose chains in aqueous solutions? *Colloids and Surfaces A: Physicochemical and Engineering Aspects, 653*, Article 130064. https://doi.org/10.1016/J.COLSURFA.2022.130064

Hill, S. E., & Prusa, K. J. (1988). Physical and sensory properties of lean ground beef patties containing methylcellulose and hydroxypropylmethylcellulose. *Journal of Food Quality, 11*(4), 331–337. https://doi.org/10.1111/j.1745-4557.1988.tb00893.x

Hinderink, E. B. A., Berton-Carabin, C. C., Schroën, K., Riaublanc, A., Houinsou-Houssou, B., Boire, A., & Genot, C. (2021). Conformational changes of whey and pea proteins upon emulsification approached by front-surface fluorescence. *Journal of Agricultural and Food Chemistry, 69*(23), 6601–6612. https://doi.org/10.1021/acs.jafc.1c01005

Janssen, S. W. P. M., Pouvreau, L., & de Vries, R. J. (2024). Commercial plant protein isolates: The effect of insoluble particles on gelation properties. *Food Hydrocolloids, 154*, Article 110049. https://doi.org/10.1016/J.FOODHYD.2024.110049

Kedzior, S. A., Dubé, M. A., & Cranston, E. D. (2017). Cellulose nanocrystals and methyl cellulose as costabilizers for nanocomposite latexes with double morphology. *ACS Sustainable Chemistry & Engineering, 5*(11), 10509–10517. https://doi.org/10.1021/acssuschemeng.7b02510

Krishina, T. G., Croy, R. R. D., & Boulter, D. (1979). Heterogeneity in subunit composition of the legumin of Pisum sativum. *Phytochemistry, 18*(11), 1879–1880. https://doi.org/10.1016/0031-9422(79)83077-0

Kundu, P. P., & Kundu, M. (2001). Effect of salts and surfactant and their doses on the gelation of extremely dilute solutions of methyl cellulose. *Polymer, 42*(5), 2015–2020. https://doi.org/10.1016/S0032-3861(00)00506-1

Kundu, P. P., & Singh, R. P. (2008). Effect of addition of surfactants on the rheology of gels from methylcellulose in N,N-dimethylformamide. *Journal of Applied Polymer Science, 108*(3), 1871–1879. https://doi.org/10.1002/APP.27839

Kyriakopoulou, K., Keppler, J. K., & van der Goot, A. J. (2021). Functionality of ingredients and additives in plant-based meat analogues. *Foods, 10*(3). https://doi.org/10.3390/foods10030600

Li, L., Liu, E., & Lim, C. H. (2007). Micro-DSC and rheological studies of interactions between methylcellulose and surfactants. *The Journal of Physical Chemistry B, 11*(23), 6410–6416. https://doi.org/10.1021/jp0712957

Li, L., Thangamathesvaran, P. M., Yue, C. Y., Tam, K. C., Hu, X., & Lam, Y. C. (2001). Gel network structure of methylcellulose in water. *Langmuir, 17*(26), 8062–8068. https://doi.org/10.1021/LA010917R

Liang, H.-F., Hong, M.-H., Ho, R.-M., Chung, C.-K., Lin, Y.-H., Chen, C.-H., & Sung, H.-W. (2004). Novel method using a temperature-sensitive polymer (Methylcellulose) to thermally gel aqueous alginate as a pH-Sensitive hydrogel. https://doi.org/10.1021/bm049813w.

Liberman, L., Schmidt, P. W., Coughlin, M. L., Ya'Akobi, A. M., Davidovich, I., Edmund, J., … Lodge, T. P. (2021). Salt-dependent structure in methylcellulose fibrillar gels. *Macromolecules, 54*(5), 2090–2100. https://doi.org/10.1021/acs.macromol.0c02429

Liu, Z., & Yao, P. (2015). Injectable thermo-responsive hydrogel composed of xanthan gum and methylcellulose double networks with shear-thinning property. *Carbohydrate Polymers, 132*, 490–498. https://doi.org/10.1016/J.CARBPOL.2015.06.013

Liu, W., Zhang, B., Lu, W. W., Li, X., Zhu, D., Yao, K. De, Wang, Q., Zhao, C., & Wang, C. (2004). A rapid temperature-responsive sol-gel reversible poly(N-isopropylacrylamide)-g-methylcellulose copolymer hydrogel. *Biomaterials, 25*(15), 3005–3012. https://doi.org/10.1016/j.biomaterials.2003.09.077

Lott, J. R., McAllister, J. W., Arvidson, S. A., Bates, F. S., & Lodge, T. P. (2013a). Fibrillar structure of methylcellulose hydrogels. *Biomacromolecules, 14*(8), 2484–2488. https://doi.org/10.1021/bm400694r.

Lott, J. R., McAllister, J. W., Wasbrough, M., Sammler, R. L., Bates, F. S., & Lodge, T. P. (2013b). Fibrillar structure in aqueous methylcellulose solutions and gels. *Macromolecules, 46*(24), 9760–9771. https://pubs.acs.org/doi/full/10.1021/ma4021642.

Martin, B. C., Minner, E. J., Wiseman, S. L., Klank, R. L., & Gilbert, R. J. (2008). Agarose and methylcellulose hydrogel blends for nerve regeneration applications. *Journal of Neural Engineering, 5*(2), 221. https://doi.org/10.1088/1741-2560/5/2/013

McAllister, J. W., Lott, J. R., Schmidt, P. W., Sammler, R. L., Bates, F. S., & Lodge, T. P. (2015a). Linear and nonlinear rheological behavior of fibrillar methylcellulose hydrogels. *ACS Macro Letters, 4*, 538–542. https://doi.org/10.1021/acsmacrolett.5b00150

McAllister, J. W., Schmidt, P. W., Dorfman, K. D., Lodge, T. P., & Bates, F. S. (2015b). Thermodynamics of aqueous methylcellulose solutions. *Macromolecules, 48*(19), 7205–7215. https://doi.org/10.1021/acs.macromol.5b01544.

Nasatto, P. L., Pignon, F., Silveira, J. L. M., Eugênia, M., Duarte, R., Noseda, M. D., & Rinaudo, M. (2015). Methylcellulose, a cellulose derivative with original physical properties and extended applications. *Polymers, 7*, 777–803. https://doi.org/10.3390/polym7050777

Pots, A. M., Gruppen, H., Hessing, M., Van Boekel, M. A. J. S., & Voragen, A. G. J. (1999). Isolation and characterization of patatin isoforms. *Journal of Agricultural and Food Chemistry, 47*(11), 4587–4592. https://doi.org/10.1021/jf981180n

Rivera del Rio, A., Opazo-Navarrete, M., Cepero-Betancourt, Y., Tabilo-Munizaga, G., Boom, R. M., & Janssen, A. E. M. (2020). Heat-induced changes in microstructure of spray-dried plant protein isolates and its implications on in vitro gastric digestion. *LWT, 118*, Article 108795. https://doi.org/10.1016/J.LWT.2019.108795

Ryu, J., & McClements, D. J. (2024). Impact of heat-set and cold-set gelling polysaccharides on potato protein gelation: Gellan gum, agar, and methylcellulose. *Food Hydrocolloids, 149*, Article 109535. https://doi.org/10.1016/J.FOODHYD.2023.109535

Sandoval, M. L., & Camerucci, M. A. (2017). Rheological behavior of aqueous mullite-albumin-methylcellulose systems. https://doi.org/10.1016/j.ceramint.2017.03.015.

Sarkar, N. (1979). Thermal gelation properties of methyl and hydroxypropyl methylcellulose. *Journal of Applied Polymer Science, 24*(4), 1073–1087. https://doi.org/10.1002/app.1979.070240420

Schmidt, P. W., Morozova, S., Ertem, S. P., Coughlin, M. L., Davidovich, I., Talmon, Y., Reineke, T. M., Bates, F. S., & Lodge, T. P. (2020). Internal structure of methylcellulose fibrils. *Macromolecules, 53*(1), 398–405. https://doi.org/10.1021/acs.macromol.9b01773

Schmidt, P. W., Morozova, S., Owens, P. M., Adden, R., Li, Y., Bates, F. S., & Lodge, T. P. (2018). Molecular weight dependence of methylcellulose fibrillar networks. *Macromolecules, 51*(19), 7767–7775. https://doi.org/10.1021/acs.macromol.8b01292

Schütz, K., Placht, A.-M., Paul, B., Brüggemeier, S., Gelinsky, M., & Lode, A. (2017). Three-dimensional plotting of a cell-laden alginate/methylcellulose blend: Towards biofabrication of tissue engineering constructs with clinically relevant dimensions. *Journal of Tissue Engineering and Regenerative Medicine, 11*, 1574–1587. https://doi.org/10.1002/term.2058

Shimoyama, T., Itoh, K., Kobayashi, M., Miyazaki, S., D'Emanuele, A., & Attwood, D. (2012). Oral liquid in situ gelling methylcellulose/alginate formulations for sustained drug delivery to dysphagic patients. *Drug Development and Industrial Pharmacy, 38*(8), 952–960. https://doi.org/10.3109/03639045.2011.634809

Sun, H., Sun, J., Dou, N., Li, J., Hussain, M. A., Ma, J., & Hou, J. (2023). Characterization and comparison of structure, thermal and functional characteristics of various commercial pea proteins. *Food Bioscience, 53*, Article 102740. https://doi.org/10.1016/J.FBIO.2023.102740

Tanger, C., Andlinger, D. J., Brümmer-Rolf, A., Engel, J., & Kulozik, U. (2021). Quantification of protein-protein interactions in highly denatured whey and potato protein gels. *MethodsX, 8*, Article 101243. https://doi.org/10.1016/J.MEX.2021.101243

Tanger, C., Quintana Ramos, P., & Kulozik, U. (2021). Comparative assessment of thermal aggregation of whey, potato, and pea protein under shear stress for microparticulation. *ACS Food Science & Technology, 1*(5), 975–985. https://doi.org/10.1021/ACSFOODSCITECH.1C00104

Tate, M. C., Shear, D. A., Hoffman, S. W., Stein, D. G., & LaPlaca, M. C. (2001). Biocompatibility of methylcellulose-based constructs designed for intracerebral gelation following experimental traumatic brain injury. *Biomaterials, 22*(10), 1113–1123. https://doi.org/10.1016/S0142-9612(00)00348-3

Thirumala, S., Gimble, J. M., & Devireddy, R. V. (2013). Methylcellulose based thermally reversible hydrogel system for tissue engineering applications. *Cells, 3*, 460–475. https://doi.org/10.3390/cells2030460

Tomšič, M., Guillot, S., Sagalowicz, L., Leser, M. E., & Glatter, O. (2009). Internally self-assembled thermoreversible gelling emulsions: ISAsomes in methylcellulose, kappa-carrageenan, and mixed hydrogels. *Langmuir: The ACS Journal of Surfaces and Colloids, 25*(16), 9525–9534. https://doi.org/10.1021/LA900766C

Tomšič, M., Prossnigg, F., & Glatter, O. (2008). A thermoreversible double gel: Characterization of a methylcellulose and κ-carrageenan mixed system in water by SAXS, DSC and rheology. *Journal of Colloid and Interface Science, 322*(1), 41–50. https://doi.org/10.1016/j.jcis.2008.03.013

Van Gelder, W. M. J. (1981). Conversion factor from nitrogen to protein for potato tuber protein. *Potato Research, 24*(4), 423–425. https://doi.org/10.1007/BF02357325/METRICS

Wang, Q., Li, L., Liu, E., Xu, Y., & Liu, J. (2006). Effects of SDS on the sol-gel transition of methylcellulose in water. *Polymer, 47*(4), 1372–1378. https://doi.org/10.1016/J.POLYMER.2005.12.049

Whistler, R. L., & BeMiller, J. N. (1992). Industrial gums: Polysaccharides and their derivatives. In *Industrial gums: Polysaccharides and their derivatives* (3rd ed., pp. 461–474). Elsevier Inc. https://doi.org/10.1016/C2009-0-03188-2.

Xu, Y., Li, L., Zheng, P., Lam, Y. C., & Hu, X. (2004). Controllable gelation of methylcellulose by a salt mixture. *Langmuir, 20*(15), 6134–6138. https://doi.org/10.1021/la049907r

Yasuda, K., Armstrong, R. C., & Cohen, R. E. (1981). Shear flow properties of concentrated solutions of linear and star branched polystyrenes. *Rheologica Acta, 20*(2), 163–178. https://doi.org/10.1007/BF01513059

Zheng, P., Li, L., Hu, X., & Zhao, X. (2004). Sol–gel transition of methylcellulose in phosphate buffer saline solutions. *Journal of Polymer Science Part B: Polymer Physics, 42*(10), 1849–1860. https://doi.org/10.1002/polb.20070